

Engineering tremella-flake-like Co_3O_4 nanostructures via a facile route for enhanced photocatalysis: rapid dye degradation

Jing Guo*, Qi Wang, Rui Wu, Xiaomei Zhao, Wenhua Gao, Weiwei Tuo, Xiaomei Ma, Yuke Gu
Ningxia Key Laboratory of Green Catalytic Materials and Technology, College of Chemistry and
Chemical Engineering, Ningxia Normal University, Guyuan 756099, China

Address correspondence to E-mail: guojingsn@163.com

1 Experiment

1.1 Materials

Cetrimonium bromide (CTAB, $C_{19}H_{42}BrN$), cobalt nitrate hexahydrate ($Co(NO_3)_2 \cdot 6H_2O$), sodium borohydride ($NaBH_4$), ethanol ($EtOH$, C_2H_6O), sodium Chloride ($NaCl$), ethylenediaminetetraacetic acid disodium salt (EDTA-2Na, $C_{10}H_{14}N_2Na_2O_8$), 2,2,6,6-tetramethyl-4-piperidinol (TEMP), 5,5-dimethyl-1-pyrroline-N-oxide (DMPO), hydrochloric acid (HCl) and sodium hydroxide ($NaOH$) were obtained from Sinopharm Chemical Reagent Co., Ltd. Rhodamine B (RhB, $C_{28}H_{31}ClN_2O_3$), peroxymonosulfate (PMS, $KHSO_5 \cdot 0.5KHSO_4 \cdot 0.5K_2SO_4$), cobalt tetraoxide (Co_3O_4), l-histidine (L-His, $C_6H_9N_3O_2$), ascorbic acid (VC, $C_6H_8O_6$) and tert-butyl alcohol (TBA, $C_4H_{10}O$) were sourced from Shanghai Macklin Biochemical Technology Co., Ltd(China). Additionally, sodium nitrate ($NaNO_3$), sodium sulfate (Na_2SO_4), sodium dihydrogen phosphate (NaH_2PO_4), disodium hydrogen phosphate (Na_2HPO_4), potassium chloride (KCl), calcium chloride ($CaCl_2$), ammonium chloride (NH_4Cl) and ferric chloride ($FeCl_3$) were also supplied by Sinopharm Chemical Reagent Co., Ltd. Zinc chloride ($ZnCl_2$) and nickel chloride hexahydrate ($NiCl_2 \cdot 6H_2O$) were acquired from Shanghai Macklin Biochemical Technology Co., Ltd (China), which methanol ($MeOH$, CH_4O) was provided by Lianlong Bohua Tianjin Pharmaceutical Chemical Co., Ltd. All chemicals were of analytical grade and used as received without further purification. Deionized (DI) water was employed throughout all experiments.

1.2 Characterization

Crystal structure of the samples was characterized by X-ray diffraction (XRD, Rigaku D/MAX 2500V, Japan) using Cu $K\alpha$ radiation ($\lambda = 1.5406 \text{ \AA}$) operated at 40 kV and 50 mA, with data collected in the 2θ range of $5-90^\circ$ at a step size of 0.02° and a scanning speed of $2^\circ/\text{min}$. Morphological and structural features were examined by field emission scanning electron microscopy (FE-SEM, ZEISS Sigma 300, Germany) and transmission electron microscopy (TEM, JEOL JEM-F200, Japan); chemical composition and elemental valence states were analyzed by X-ray photoelectron spectroscopy (XPS, Thermo Scientific K-Alpha, USA). Fourier transform infrared (FT-

IR) spectra were recorded on a Nicolet 6700 spectrometer to identify functional groups and chemical bonds. The concentration of RhB during the photocatalytic process was monitored using a UV–Vis spectrophotometer (P4, MAPADA, Shanghai). Specific surface area was determined by nitrogen adsorption–desorption measurements at 77 K on a Micromeritics 3020 analyzer, and the Bruner–Emmett–Teller (BET) method was applied for calculation. The leaching of cobalt ions from the solution was analyzed using inductively coupled plasma-optical emission spectrometer (ICP-OES, Agilent 5110). Degradation intermediates were analyzed using the chromatographic column Waters BEH C18 (2.1×100 mm, 1.7 μm) in combination with a high-performance liquid chromatography-mass spectroscopy (HPLC-MS) system. A formic acid aqueous solution (0.1%) was used as the mobile phase A, and an acetonitrile solution was used as the mobile phase B; the flow rate was set at 0.3 mL·min⁻¹. The injection volume of the liquid was 5 μL, and the scanning range was controlled from 50 to 1000 m/z. The sheath gas temperature and flow were set at 350°C and 12 L·min⁻¹, respectively.

1.3 Measurement of photocatalytic activity

The photocatalytic performance of the synthesized samples was evaluated by degrading rhodamine B (RhB, 50 mL, 20 mg·L⁻¹) under visible-light irradiation ($\lambda > 420$ nm) from a 300 W xenon lamp. Prior to irradiation, the suspension was magnetically stirred in the dark for 30 min to establish adsorption–desorption equilibrium. During the irradiation process, approximately 3 mL of the suspension was sampled at regular intervals and immediately filtered through a 0.22 μm polytetrafluoroethylene membrane. Concentration of RhB in the filtrate was determined by UV–Vis spectroscopy. Degradation efficiency (R) was calculated using the following equation: $R (\%) = ((C_0 - C_t)/C_0) \times 100\%$, where C_0 denotes the concentration of pollutants in the initial sample, and C_t represents the concentration in the sample after photodegradation, measured at a given sampling.¹⁻³

2 Results and Discussions

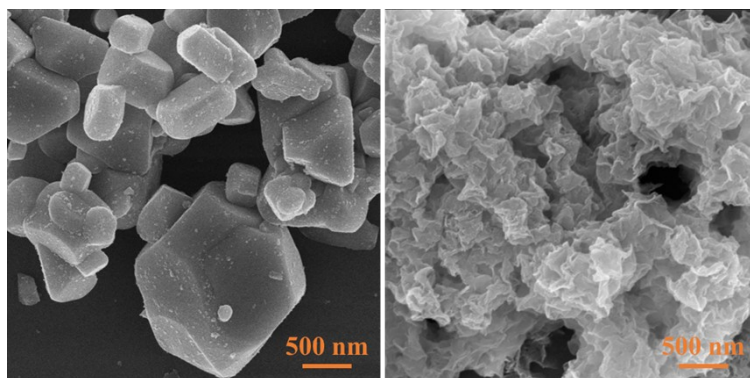


Fig. S1 SEM images of (a) Co₃O₄-M, (b) Co₃O₄-P

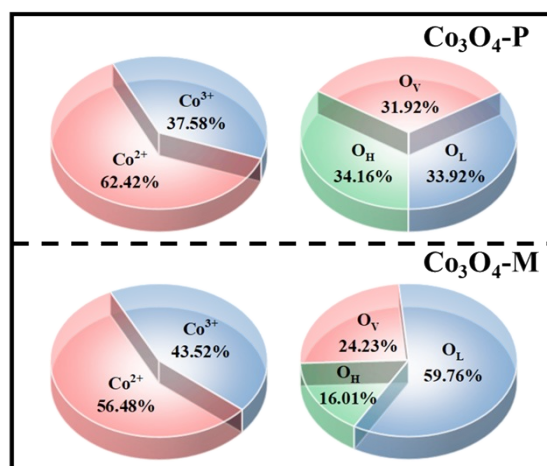


Fig. S2 Fractions of Co and O species in $\text{Co}_3\text{O}_4\text{-P}$ and $\text{Co}_3\text{O}_4\text{-M}$

Table S1 S_{BET} , pore volume and pore size of the prepared samples

Samples	S_{BET} ($\text{m}^2 \cdot \text{g}^{-1}$)	V_{p} ($\text{cm}^3 \cdot \text{g}^{-1}$)	Pore Diameter (nm)
$\text{Co}_3\text{O}_4\text{-P}$	210.8	1.154	21.898
$\text{Co}_3\text{O}_4\text{-M}$	11.4	0.030	10.488

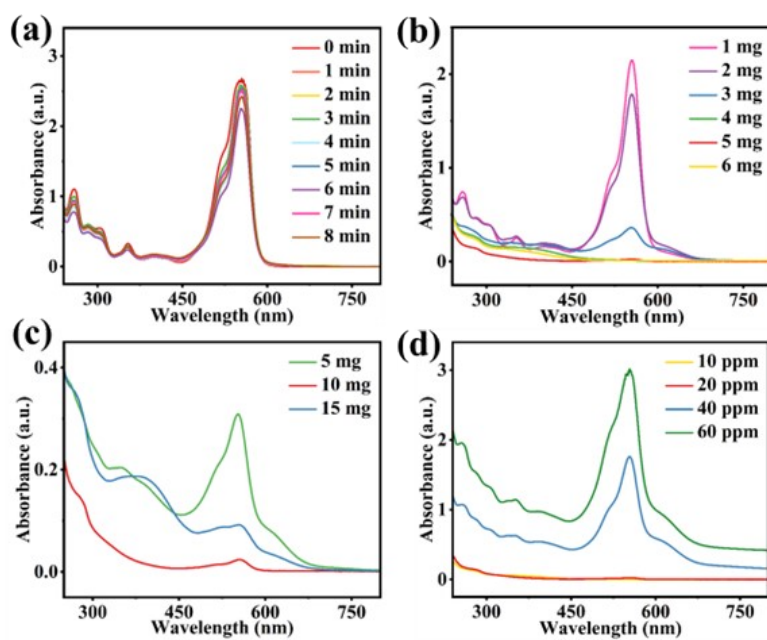


Fig. S3 UV-Vis absorption spectra of RhB solutions under different reaction conditions: (a) $\text{Co}_3\text{O}_4\text{-M}$, (b) catalyst dosage, (c) PMS dosage, and (d) RhB concentration

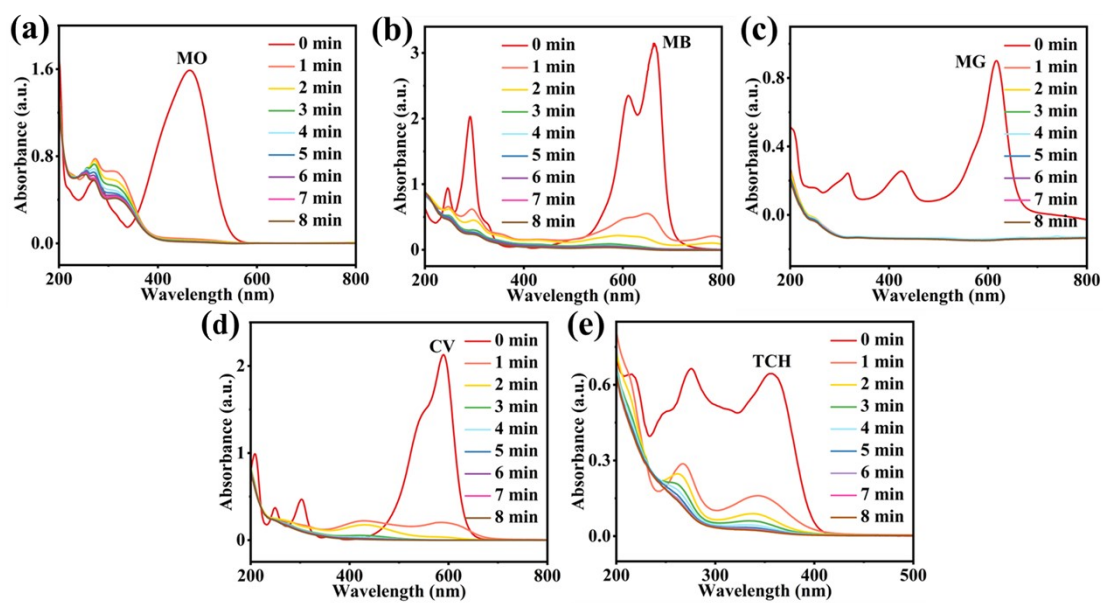


Fig. S4 UV-Vis absorption spectra for (a) MO, (b)MB, (c)MG, (d)CV, and (e)TCH degradation under light irradiation

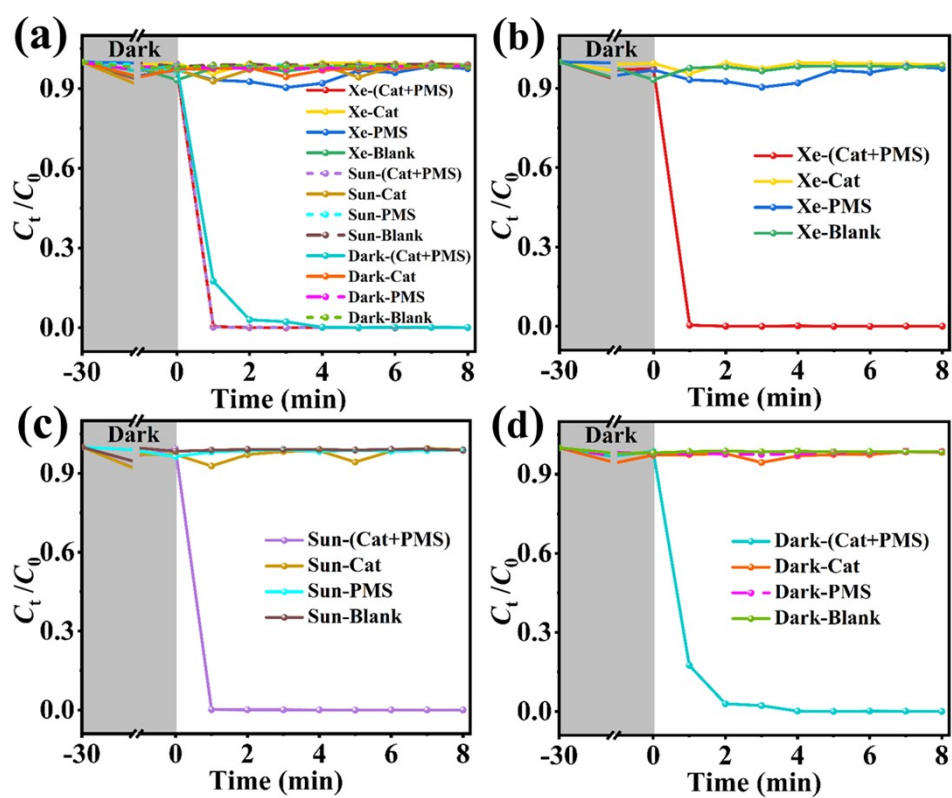


Fig. S5 Effect of light source on RhB degradation activity: (a) different light sources (comparison), (b) visible light, (c) sunlight, and (d) dark condition

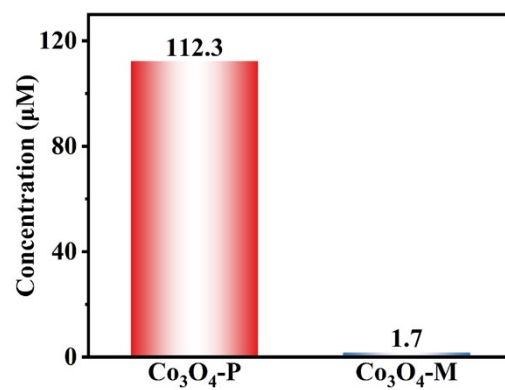


Fig. S6 Metal ion leaching of Co₃O₄-P and Co₃O₄-M

Table S2 Comparison of photodegradation performance with previously reported catalysts

Catalysts	Cat. Conc. (g·L ⁻¹)	P. Conc. (mg·L ⁻¹)	PMS (mM)	Time (min)	<i>D</i> (%)	<i>k</i> (min ⁻¹)	Ref.
Co ₃ O ₄ -S	1.0	20 (NFX)	1.0	40	92.4%	0.2558	4
Bi ₂ Fe ₄ O ₉ -LA	0.3	10 (DMP)	1.0	60	94.7%	0.0542	5
FeS ₂	0.03	20 (QNC)	1.0	30	100.0%	0.4585	6
Fe ₂ O ₃ /VO ₂	0.1	5 (SCP)	0.25	30	100.0%	0.8312	7
B-CuO	1.2	4 (IBP)	0.3	30	92.9%	0.1300	8
Co ₃ O ₄ -CuO	0.2	20 (LEV)	5.2	60	97.0%	2.0851	9
Mn ₃ O _{4-x}	0.1	20 (BPA)	0.5	15	100.0%	0.2580	10
TiO ₂	0.05	50 (PFOA)	1.0	480	99.6%	0.0052	11
Co ₃ O ₄ -P	0.1	20 (RhB)	1.0	1	99.6%	5.4440	This work

Cat. Conc., Catalyst Concentration; P. Conc., Pollutants Concentration; *D*, Degradation efficiency; NFX, norfloxacin; DMP, dimethyl phthalate; QNC, quinclorac; SCP, sulfachloropyridazine; IBP, ibuprofen; LEV, levofloxacin; BPA, bisphenol A; PFOA perfluorooctanoic acid; Ref., reference.

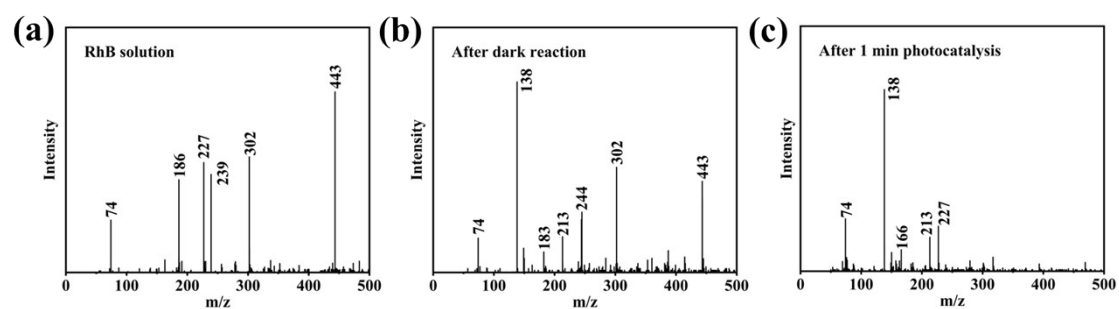
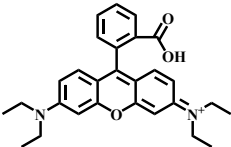
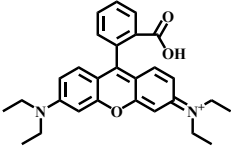
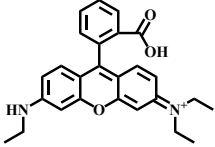
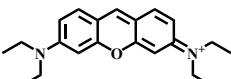
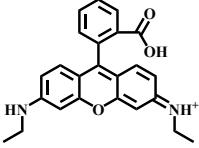
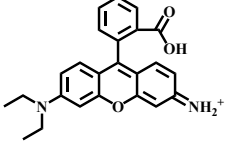
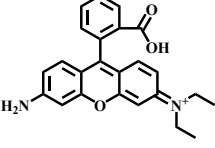
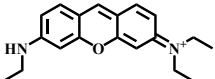
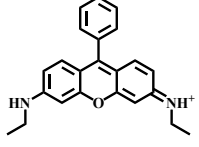
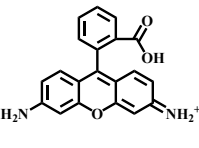
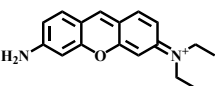
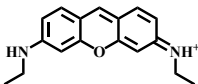
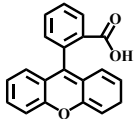
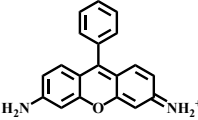
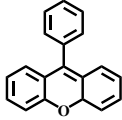
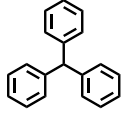
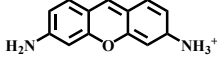
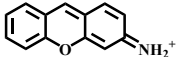
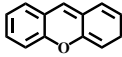
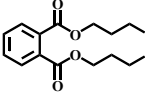
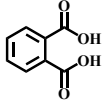
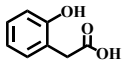
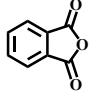
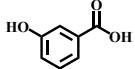
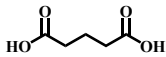

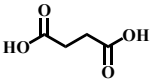
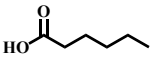
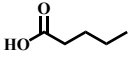

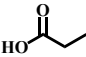
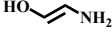


Fig. S7 The HPLC-MS spectra of the solution samples during the RhB degradation

Table S3 Identification of RhB for Co₃O₄-P degradation intermediates by HPLC-MS

Compound	Structure	Formula	m/z
		C ₂₈ H ₃₁ N ₂ O ₃ ⁺	443
P1		C ₂₆ H ₂₇ N ₂ O ₃ ⁺	415
P2		C ₂₆ H ₂₇ N ₂ O ₃ ⁺	415
P3		C ₂₁ H ₂₇ N ₂ O ⁺	323
P4		C ₂₄ H ₂₃ N ₂ O ₃ ⁺	387
P5		C ₂₄ H ₂₃ N ₂ O ₃ ⁺	387
P6		C ₂₄ H ₂₃ N ₂ O ₃ ⁺	387
P7		C ₁₉ H ₂₃ N ₂ O ⁺	387
P8		C ₂₃ H ₂₃ N ₂ O ⁺	343
P9		C ₂₀ H ₁₅ N ₂ O ₃ ⁺	302
P10		C ₁₇ H ₁₉ N ₂ O ⁺	267

P11		$C_{17}H_{19}N_2O^+$	267
P12		$C_{20}H_{14}O_3$	302
P13		$C_{19}H_{15}N_2O^+$	287
P14		$C_{19}H_{14}O$	258
P15		$C_{19}H_{16}$	244
P16		$C_{13}H_{13}N_2O^+$	213
P17		$C_{13}H_{10}NO^+$	196
P18		$C_{13}H_{10}O$	182
P19		$C_{16}H_{22}O_4$	278
P20		$C_8H_6O_4$	166
P21		$C_8H_8O_3$	152
P22		$C_8H_4O_3$	148
P23		$C_7H_6O_3$	138
P24		$C_5H_8O_4$	132

P25		C ₉ H ₂₀	128
P26		C ₅ H ₈ O ₃	118
P27		C ₅ H ₈ O ₃	116
P28		C ₅ H ₈ O ₃	102
P29		C ₇ H ₁₆	100
P30		C ₅ H ₁₀ O	74
P31		C ₄ H ₉ N	59

Reference

1. F. Qiu, Y. Pan, L. Wang, H. Song, X. Liu, Y. Fan and S. Zhang, *Sep. Purif. Technol.*, 2024, **330**, 125139.
2. H. Salehzadeh, M.J. Rezaei, B. Shahmoradi, B. Nikkhoo, A. Allahweisi, A. Maleki, B. Rahimi, M. Rezaee, K. Nasiri and H.-J. Choi, *J. Environ. Manage.*, 2025, **386**, 125710.
3. L.R. Jabbar, S.H. Ammar and A.A. Amooey, *J. Water Process. Eng.*, 2025, **77**, 108545.
4. J. Song, X. Ren, G. Hu, X. Hu and W. Cheng, *PROCESS SAF ENVIRON*, 2023, **176**, 140-154.
5. J. Ding, H. Yin, X. Li, X. Yao, Q. Wang, H. Yang, H. Lv, L.-z. Budazhapov and J. Wang, *Chem. Eng. J.*, 2025, **507**, 160497.
6. M.e. Zhong, Z. Wen, J. Ouyang, Z. Liu, Y. Liu, F. Jiang, L. Chen, C. Ding and B. Ji, *J. Environ. Chem. Eng.*, 2025, **13**, 117930.
7. Y. Chai, Q. Wang, X. Zhang, L. Dong, M. Zhang, P. Rao and N. Gao, *J. Water Process Eng.*, 2025, **78**, 108602.
8. C. Tan, Y. Huang, X. Lin, P. Li, L. Su and Q. Wang, *J. Water Process Eng.*, 2025, **69**, 106711.
9. X. Jia, H. He, X. Zhao, Y. Li, C. Wang, Y. Yang and J. Wu, *New J. Chem.*, 2024,

48, 14801-14812.

10. J. Wu, H. Xie, G. Zhang, H. Lin, J. Xing, L. Wang and J. Xu, *Chem. Eng. J.*, 2024, **499**, 156402.
11. B. Xu, M.B. Ahmed, J.L. Zhou and A. Altaee, *CHEMOSPHERE*, 2020, **243**, 125366.